

Noise figure and photon statistics in coherent anti-Stokes Raman scattering

D. Dimitropoulos, D. R. Solli, R. Claps, and B. Jalali

University of California, Los Angeles, CA 90095-1594

jalali@ucla.edu

<http://www.ee.ucla.edu/~oecs/>

Abstract: Coherent anti-Stokes Raman scattering (CARS) is a well-known Raman scattering process that occurs when Stokes, anti-Stokes and pump waves are properly phase-matched. Using a quantum-field approach with Langevin noise sources, we calculate the noise figure for wavelength conversion between the Stokes and anti-Stokes waves in CARS and show its dependence on phase mismatch. Under phase matched conditions, the minimum noise figure is approximately 3 dB, with a correction that depends on the pump frequency, Stokes shift, refractive indices, and nonlinear susceptibilities. We calculate the photon statistics of CARS and show that the photon number distribution is non-Gaussian. Our findings may be significant for currently pursued applications of CARS including wavelength conversion in data transmission and spectroscopic detection of dilute biochemical species.

©2006 Optical Society of America

OCIS codes: (270.5290) Photon Statistics; (190.2620) Frequency conversion; (190.4410) Nonlinear optics, parametric processes; (190.5650) Raman Effect

References and links

1. P.D. Maker, R.W. Terhune, "Study of optical effects due to an induced polarization third order in the electric field strength," *Phys. Rev.* **137**, A801 (1965).
2. H. Vogt, "Coherent and hyper-Raman techniques" in *Topics in Applied Physics* (eds. M. Cardona, G. Guntherodt) vol. **50**, p. 207, Springer-Verlag (1982).
3. A.M. Zheltikov, P. Radi, "Non-linear Raman spectroscopy 75 years after the Nobel Prize for the discovery of Raman scattering and 40 years after the first CARS experiments," *J. of Raman Spectrosc.* **36**, 92-4 (2005).
4. G. Beadie, Z.E. Sariyanni, Y. V. Rostovtsev, T. Opatrny, J. Reintjes, M.O. Scully, "Towards a FAST CARS anthrax detector: coherence preparation using simultaneous femtosecond laser pulses," *Opt. Commun.* **244**, 423-430 (2005).
5. K.P. Knutsen, J.C. Johnson, A.E. Miller, P.B. Petersen, R.J. Saykally, "High-spectral-resolution multiplex CARS spectroscopy using chirped pulses," *SPIE Proc.* **5323**, 230-9 (2004).
6. K. Ishii, H. Hamaguchi, "Picosecond time-resolved multiplex CARS spectroscopy using optical Kerr gating," *Chem. Phys. Lett.* **367**, 672-7 (2003).
7. E.O. Potma, C.L. Evans, X.S. Xie, "Heterodyne coherent anti-Stokes Raman scattering (CARS) imaging," *Opt. Lett.* **31**, 241-3 (2006).
8. F. Vestin, M. Afzelius, C. Brackmann, P-E. Bengtsson, "Dual-broadband rotational CARS thermometry in the product gas of hydrocarbon flames," *Proc. of the Combustion Inst.* **30**, 1673-80 (2004).
9. N. Djaker, P-F. Lenne, H. Rigneault, "Vibrational imaging by coherent anti-Stokes Raman scattering (CARS) microscopy," *SPIE Proc.* **5463**, 133-9 (2004).
10. R. Claps, V. Raghunathan, D. Dimitropoulos, B. Jalali, "Anti-Stokes Raman conversion in Silicon waveguides," *Opt. Express* **11**, 2862 - 2872 (2003).
11. J. Perina, "Photon statistics in Raman scattering with frequency mismatch," *Optica Acta* **28**, 1529 (1981).
12. J. Perina, "Photon statistics in Raman scattering of intense coherent light," *Optica Acta* **28**, 325 (1981).
13. M. Karska, J. Perina, "Photon statistics in stimulated Raman scattering of squeeze light," *J. Mod. Optics* **37**, 195 (1990).
14. P.L. Voss, P. Kumar, "Raman-noise-induced noise-figure limit for $\chi^{(3)}$ parametric amplifiers," *Opt. Lett.* **29**, 445 (2004).

15. R. Tang, P.L. Voss, J. Lasri, P. Devgan, P. Kumar, "Noise-figure of fiber-optical parametric amplifiers and wavelength converters: experimental investigation," *Opt. Lett.* **29**, 2372 (2004).
 16. K.K. Das, G. S. Agarwal, Y.M. Golubev, M.O. Scully, "Langevin analysis of fundamental noise limits in coherent anti-Stokes Raman spectroscopy," *Phys. Rev. A* **71**, 013802 (2005).
 17. R.W. Boyd, *Nonlinear Optics*, 3rd ed. (Academic Press, 1992).
 18. A. Yariv, *Quantum Electronics*, 3rd ed. (Wiley: New York 1989), Chapter 5.
 19. H.A. Haus, *Electromagnetic Noise and Quantum Optical Measurement* (Springer 2000), p. 217 – 223.
 20. W.H. Louisell, *Quantum Statistical Properties of Radiation* (John Wiley & Sons 1973).
-

1. Introduction

Coherent anti-Stokes Raman scattering (CARS) is a nonlinear optical process in which energy is parametrically transferred between phase-matched Stokes and anti-Stokes fields via interaction with vibrational modes of the material in the presence of a strong pump wave. Since its discovery by Maker and Terhune in the early days of nonlinear optical research [1], it has found numerous applications in spectroscopy and substance identification [2,3] and continues as an active field of applied research [4-9]. CARS was also recently demonstrated in silicon and has been proposed as means of wavelength conversion between the technologically important 1300 nm and the 1550 nm wavelength bands [10].

An important topic that has been discussed is the fundamental noise in the CARS process. To our knowledge, the first investigation to address the issue of noise in CARS was conducted by Perina et al [11-13] with more recent investigations due to Voss et al [14-15]. Scully et al [16] have also addressed this issue in the context of an ultra-fast spectroscopic technique they proposed for detection of rarified bacterial spores [4]. In References [11-13], the photon statistics were calculated for the CARS process, but the treatment is in the time-domain. The treatment in [16] is also in the time-domain. Voss et al used spatial propagation equations for the optical fields and calculated the noise figure for Raman amplification and CARS [14-15], but did not calculate the photon statistics.

In this paper, we formulate the problem using spatial propagation equations and obtain both the noise figure and, for the first time, the photon statistics using such an approach. Although the time-domain approach is appropriate for cavity dynamics, this spatial treatment is more suitable for treating waveguide propagation where the effects of waveguide and material dispersion, as well as phase mismatch are explicitly included. We obtain the propagation equations for Stokes and anti-Stokes fields in a different manner than that employed in [14-15]. We demonstrate that the minimum noise figure obtained at perfect phase matching is close to 3 dB, but deviates from this value by a factor that depends on the contribution of both linear and nonlinear dispersion, as well as the Stokes shift and pump frequency. There are two distinct contributions to the noise in the output signal: (1) noise originating from the zero point fluctuations of the inputs and (2) noise originating from the coupling of the Stokes and anti-Stokes fields with the damped material vibrations. We also calculate the full photon probability distribution at the output wavelength, and show that its tails deviate significantly from those of the Gaussian distribution. These findings may be important for determining the minimum bit error rate (BER) in CARS data transfer, as well as the fundamental detection limit of CARS spectroscopy.

We start with the classical equations for CARS and convert them into propagation equations for the quantum field operators for the Stokes and anti-Stokes modes. Using these equations, we derive the noise sources for the Stokes and the anti-Stokes fields by imposing the requirement that the commutators of their field operators must be conserved. Throughout the paper we deal with an ideal medium that does not have optical losses or permit other nonlinear optical processes. Optical losses (linear or nonlinear) can be easily included numerically, but are not discussed here because they are not fundamental to the CARS process.

2. Equations of motion

The CARS process increases the noise in both the Stokes and anti-Stokes fields. These modes are coupled together through interaction with the damped vibrational phonons of the material and since CARS involves dissipative interactions, it must introduce noise into the optical signals. The propagation of the Stokes and anti-Stokes field operators (denoted \hat{a}_S and \hat{a}_{AS} respectively), including the effect of this excess noise (using the Langevin noise operators $\hat{N}(x)$, $\hat{N}^+(x)$ discussed below) are described by the following two equations:

$$\frac{d\hat{a}_S}{dx} = g_S \hat{a}_S + r g_S \exp(j(\Delta\beta x + 2\varphi_P)) \hat{a}_{AS}^+ - j\sqrt{2g_S} \hat{N}^+ \quad (1a)$$

$$\begin{aligned} \frac{d\hat{a}_{AS}^+}{dx} = & -r^2 g_S \hat{a}_{AS}^+ - r g_S \exp(-j(\Delta\beta \cdot x + 2\varphi_P)) \hat{a}_S \\ & + j \exp(-j(\Delta\beta \cdot x + 2\varphi_P)) \sqrt{2r^2 g_S} \hat{N}^+. \end{aligned} \quad (1b)$$

These equations are derived in Appendix A starting from the classical field-amplitude equations of CARS, replacing the field amplitudes with quantum field operators, and invoking the principle of “commutator conservation.” In the above equations the operators that appear obey the following commutation relationships: $[\hat{a}_S, \hat{a}_S^+] = 1$, $[\hat{a}_{AS}, \hat{a}_{AS}^+] = 1$, $[\hat{a}_S, \hat{a}_{AS}^+] = 0$ and, since the noise is uncorrelated at each spatial point, $[\hat{N}(x), \hat{N}^+(x')] = \delta(x - x')$. The quantity $\Delta\beta = 2\beta_P - \beta_S - \beta_{AS}$ is the wavevector mismatch between the waves (β_j is the propagation constant of the j -th wave, with $j = P, S$ or AS), g_S is equal to one half of the Raman (power) gain coefficient, φ_P is the phase of the pump wave and $r = \frac{\omega_{AS} n_S (\chi_{AS}^* / \chi_S)^{1/2}}{\omega_S n_{AS}}$, where ω_S, ω_{AS} are Stokes and anti-Stokes frequencies, n_S, n_{AS} the indices of refraction and χ_S, χ_{AS}^* are the Raman susceptibilities. Since we will be interested in a narrow frequency band around the center of the Raman resonance, g_S and r are real quantities.

The above equations (1a) and (1b) have the property that they conserve the commutators of the Stokes and anti-Stokes fields along propagation in the x -direction, so that for example, $[\hat{a}_S(x), \hat{a}_S^+(x)] = [\hat{a}_S(x'), \hat{a}_S^+(x')]$. This is achieved in the equations through the presence of the terms involving the “Langevin noise source operators” $\hat{N}(x)$, $\hat{N}^+(x)$, which introduce fluctuations in the Stokes and anti-Stokes fields, as described in more detail below.

The general solution to the above equations is:

$$\hat{a}_S(x) = A(x)\hat{a}_S(0) + B(x)\hat{a}_{AS}^+(0) + \int_0^x dx' N_S(x-x')\hat{N}^+(x') \quad (2a)$$

$$\hat{a}_{AS}^+(x) = C(x)\hat{a}_{AS}^+(0) + D(x)\hat{a}_S(0) + \int_0^x dx' N_{AS}(x-x')\hat{N}^+(x'). \quad (2b)$$

The details to the above solution along with general expressions for the A, B, C and D coefficients are presented in full in Appendix B.

3. Wavelength conversion noise figure

We can now calculate the fluctuations of the Stokes (anti-Stokes) field at the output $x = L$ of the wavelength converter, when there is anti-Stokes (Stokes) field present at the input $x = 0$. Let us consider, for example, the case where there are no photons at the Stokes frequency and the anti-Stokes wave at the input is a coherent state. The assumption of zero photons in the Stokes input is a good one, since at room temperature the mean photon number of the thermal optical radiation is practically zero. In our notation, $| \rangle_S, | \rangle_{AS}$ denotes the states of the Stokes and anti-Stokes inputs, respectively.

At this point we need to discuss the concept of the noise reservoir “states.” At every point x in the waveguide, the state of the reservoir is denoted by $| \rangle_{R,x}$ (the states on which the operators $\hat{N}(x)$ and $\hat{N}^+(x)$ act). To simplify the notation we will use the combined state $| \rangle_R = \prod_x | \rangle_{R,x}$ in the calculations. Since the noise reservoir creates fluctuations in the vibrational mode with which the optical waves interact, the frequency of the reservoir is that of the material vibrations. The noise sources originate from the fluctuations in the vibrational modes being “upconverted” to the Stokes and anti-Stokes frequencies due to interaction with the optical pump wave. To show this, one takes the noise reservoir to be a thermal density matrix and calculates the mean Stokes photon number in the case $\Delta\beta \gg g_S$ (where Stokes and anti-Stokes are uncoupled) when there is no input at $x = 0$. This gives the Stokes spontaneous emission rate, which is proportional to the mean number of reservoir quanta plus one. Since we know that the Stokes spontaneous emission rate is also proportional to the mean phonon number plus one, we can identify the reservoir frequency with the vibrational mode frequency. We will assume next that the noise reservoir is in the ground state ($kT \ll \hbar\omega_{VIB}$).

We will calculate the noise figure first for the case of anti-Stokes to Stokes conversion when the anti-Stokes input is a coherent state of amplitude a . This situation corresponds to the state $|0\rangle_S |a\rangle_{AS} |0\rangle_R$ and the mean input photon number in the anti-Stokes field is $|a|^2$.

Referring to Eqs. (2a) and (2b), we can express the mean photon rate at the Stokes output as:

$$\langle \hat{a}_S^+(x) \hat{a}_S(x) \rangle = \underbrace{|B(x)|^2 |a|^2}_{\text{Converted signal}} + \underbrace{|B(x)|^2 + N_{S,TOT}}_{\text{d.c. term}}, \quad (3)$$

where $N_{S,TOT} = \int_0^x dx' |N_S(x')|^2$. For the fluctuations in photon number we find:

$$\begin{aligned} \langle \Delta(\hat{a}_S^+(x) \hat{a}_S(x))^2 \rangle = & |B(x)|^2 (N_{S,TOT} + |A(x)|^2 + |B(x)|^2) |a|^2 \\ & + |A(x)|^2 (|B(x)|^2 + N_{S,TOT}). \end{aligned} \quad (4)$$

So far we have discussed single frequency signals; if the photons are sent in a pulse of spectral width Δf , then $|a|^2 = R / \Delta f$, where R is the input photon rate. The optical (signal-to-noise ratio) *SNR* for an ideal photodetector is:

$$\begin{aligned}
SNR(x) &= \frac{\left\langle \left(\hat{a}_s^+(x) \hat{a}_s(x) \right)_{\text{SIGNAL}} \right\rangle^2}{\left\langle \Delta \left(\hat{a}_s^+(x) \hat{a}_s(x) \right)^2 \right\rangle} \\
&= \frac{|B(x)|^2 R^2}{|B(x)|^2 (N_{s,TOT} + |A(x)|^2 + |B(x)|^2) R \cdot \Delta f + |A(x)|^2 (|B(x)|^2 + N_{s,TOT}) (\Delta f)^2}.
\end{aligned} \tag{5}$$

The noise figure F of the wavelength conversion process is:

$$\begin{aligned}
F_{AS \rightarrow S} &= \frac{SNR(0)}{SNR(L)} = \frac{R / \Delta f}{SNR(L)} \\
&= 1 + \frac{N_{s,TOT} + |A(L)|^2}{|B(L)|^2} + \frac{|A(L)|^2 (|B(L)|^2 + N_{s,TOT})}{|B(L)|^2 (R / \Delta f)},
\end{aligned} \tag{6}$$

where the anti-Stokes input wave shot noise has been used as the reference. In the limit of a large input signal the minimum noise figure reduces to:

$$F_{AS \rightarrow S, MIN} = 1 + \frac{N_{s,TOT} + |A(L)|^2}{|B(L)|^2}. \tag{7}$$

On the other hand, the noise figure of Stokes to anti-Stokes conversion is given by:

$$F_{S \rightarrow AS} = 1 + \frac{|C(L)|^2 + N_{AS,TOT}}{|D(L)|^2} \left(1 + \frac{1}{R / \Delta f} \right), \tag{8}$$

where $N_{AS,TOT} = \int_0^x dx' |N_{AS}(x)|^2$. In the limit of a large input signal, this expression reduces to:

$$F_{S \rightarrow AS, MIN} = 1 + \frac{|C(L)|^2 + N_{AS,TOT}}{|D(L)|^2}. \tag{9}$$

Equations (7) and (9) provide a physical picture of the origin of the noise in the CARS conversion process. The excess noise figure has two parts. In the anti-Stokes to Stokes conversion, for example, the term proportional to $|A(L)|^2$ originates from the zero-point fluctuations of the Stokes input, which propagates from $x = 0$ to $x = L$ while mixing with the converted signal. On the other hand, the term proportional to $N_{AS,TOT}$ quantifies the noise from the material vibrations that are coupled to the Stokes wave and the converted signal.

As an example, next we will calculate the noise figure in the case of perfect phase-matching ($\Delta\beta = 0$) with $\varphi_p = 0$; the relevant coefficients are given in the Appendix B in Eqs. (B9) and (B10). There are two regimes in which we are interested. The first case is when $g_s x \gg 1$ with $g_s (r^2 - 1)x \ll 1$, which gives $|A(x)|^2 \approx (1 + g_s x)^2$, $|B(x)|^2 \approx (r g_s x)^2$ and $N_{s,TOT} \approx 2 g_s x$. In this case, the minimum noise figure becomes:

$$F_{AS \rightarrow S, MIN} = 1 + (1/r^2) \cong 2, \tag{10}$$

which is close to the minimum noise figure of an optical amplifier.

The second case is when $g_s(r^2 - 1)x \gg 1$ and the conversion efficiency saturates. In this case, $|A(x)|^2 \approx \frac{r^4}{(r^2 - 1)^2}$, $|B(x)|^2 \approx \frac{r^2}{(r^2 - 1)^2}$ and $N_{s,TOT} \approx \frac{1}{(r^2 - 1)}$, so the minimum noise figure reduces to:

$$F_{AS \rightarrow S, MIN} = 2 + r^2 - (1/r^2) \approx 2. \quad (11)$$

These expressions deviate from the ideal amplifier by a factor which depends on the ratio of the photon energies of the Stokes and anti-Stokes waves, as well as the difference in their indices of refraction and their nonlinear susceptibilities. In the case of $\Delta\beta = 0$ for Stokes to anti-Stokes conversion, we have the following limiting values for the noise figure:

$$F_{S \rightarrow AS, MIN} = \begin{cases} 2 + \frac{1}{(rg_s x)^2}, & g_s(r^2 - 1)x \ll 1 \\ 2 + \frac{(r^2 - 1)^2}{r^2}, & g_s(r^2 - 1)x \gg 1. \end{cases} \quad (12)$$

In Fig. 1, we display the noise figure vs. pump intensity for the Stokes to anti-Stokes and anti-Stokes to Stokes conversion processes for perfect phase matching with an interaction length L of 2 cm, $2g_s = (30 \text{ cm/GW}) \times I_p$ and $r = 1.2$ (typical parameters for semiconductor Raman media). We note that the curves for the two processes are qualitatively similar, converging in the weak pump limit, and asymptotically approaching the limiting value near 3 dB in the strong pump regime. When the intensity is low the noise figure is heavily impaired due to the low conversion gain, but at high intensity the quantum noise approaches a limit similar to the 3 dB minimum in amplifiers.

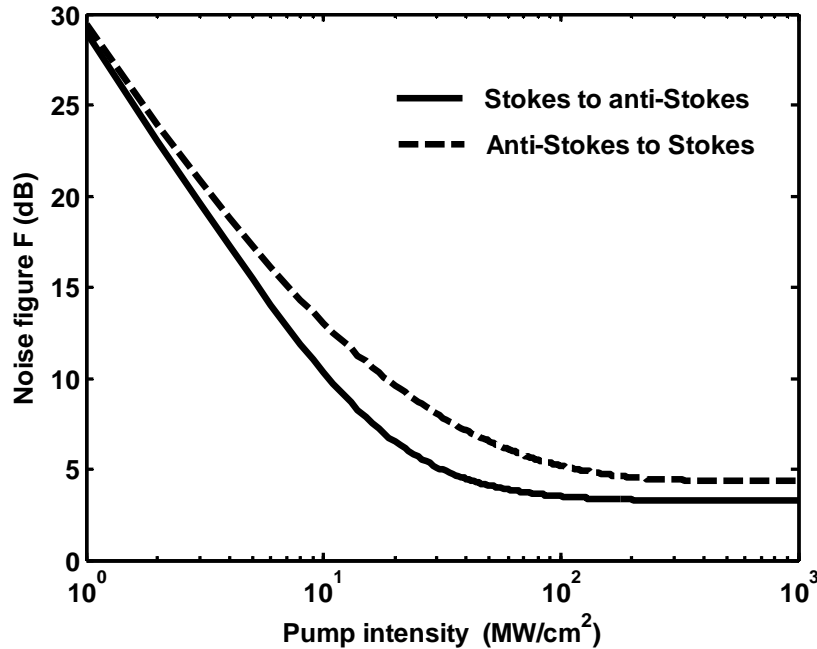


Fig. 1. The noise figure for signal conversion with perfect phase-matching is shown for interaction length $L = 2$ cm, a gain coefficient $2g_s = (30 \text{ cm/GW}) \times I_p$ and $r = 1.2$.

We have also plotted the noise figure for both Stokes to anti-Stokes and anti-Stokes to Stokes conversion as a function of the phase-mismatch, with $r = 1.2$, $g_s = 0.25 \text{ cm}^{-1}$ (which translates to a gain coefficient of 0.5 cm^{-1}) and $L = 2 \text{ cm}$ (see Fig. 2). Interestingly, the noise figure rapidly becomes large as the phase mismatch is increased, yet also shows periodic undulations corresponding with the well-known relationship between CARS efficiency and phase mismatch.

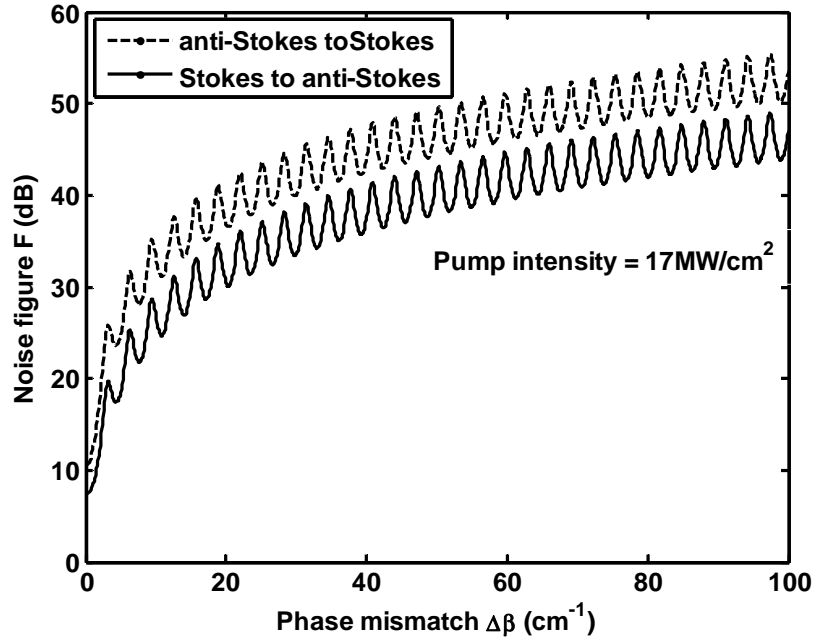


Fig. 2. The noise figure variation with the phase-mismatch for both Stokes and anti-Stokes scattering with $L = 2 \text{ cm}$, $r = 1.2$, a gain coefficient 30 cm/GW and a pump intensity of 17 MW/cm^2 ($g_s = 0.25 \text{ cm}^{-1}$).

4. Photon number distribution

We have also calculated the photon-number distribution for anti-Stokes (Stokes) photons at the output when the Stokes (anti-Stokes) field at the input is a coherent state. To perform the calculation we assume the “lumped” input-output relationships:

$$\hat{a}_s(x) = A\hat{a}_s(0) + B\hat{a}_{AS}^+(0) + N_s\hat{N}^+ \quad (13a)$$

$$\hat{a}_{AS}^+(x) = D\hat{a}_s(0) + C\hat{a}_{AS}^+(0) + N_{AS}\hat{N}^+, \quad (13b)$$

with the commutator $[\hat{N}, \hat{N}^+] = 1$. The quantity $|N_s|^2$ equals the quantity $N_{S,TOT}$ in Section 4 of the paper and $|N_{AS}|^2$ equals $N_{AS,TOT}$. The quantities A, B, C, D are the same quantities that appear in equations (2a) and (2b). Formulated in this way, the lumped description of (13a) and (13b) gives the same results as the description of (1a) and (1b).

To derive the photon statistics, we assume that the reservoir is in a thermal state with the following density matrix:

$$\hat{\rho} = (1-q) \sum_{n=0}^{\infty} q^n |n\rangle_{RR} \langle n|, \quad (14)$$

where $q = \langle n \rangle_R / (1 + \langle n \rangle_R)$ and $\langle n \rangle_R$ is the thermal occupation number of the reservoir. The probability distribution for both Stokes to anti-Stokes conversion and anti-Stokes to Stokes conversion has the following form:

$$p(n_o) = e^{-\mu|a|^2} (1-\lambda) \lambda^{n_o} L_{n_o} \left(\frac{\mu|a|^2(\lambda-1)}{\lambda} \right), \quad (15)$$

where $L_{n_o}(x) = \sum_{n=0}^{n_o} \binom{n_o}{n} \frac{(-x)^n}{n!}$ is the Laguerre polynomial of order n_o and $|a|^2$ is the mean photon number of the input coherent state. For Stokes to anti-Stokes conversion $\mu/\lambda = |D|^2 / (u + |D|^2)$ and $\lambda = (u + |D|^2) / (1 + u + |D|^2)$ with $u = |N_{AS}|^2 q / (1-q)$, whereas, for anti-Stokes to Stokes conversion $\mu/\lambda = |B|^2 / (u' + |B|^2)$ and $\lambda = (u' + |B|^2) / (1 + u' + |B|^2)$ with $u' = |N_S|^2 / (1-q)$. The distribution has the mean value: $\langle n_o \rangle = (\lambda + \mu|a|^2) / (1-\lambda)$. A derivation of this result for the simplified case where the reservoir is in the ground state is presented in Appendix C. Notice that when there is no input signal ($a=0$) the photon distribution in Eq. (15) becomes a thermal distribution; the spontaneously emitted Stokes and anti-Stokes fields in CARS have thermal distributions with a temperature that is determined by the parameter λ .

In Fig. 3, we show a representative plot of the probability distribution for anti-Stokes to Stokes conversion in the case of a coherent state input with a mean photon number of 400. This input yields a mean output photon number 45; for comparison, we have also plotted a Gaussian distribution with this mean value, illustrating that the tails of the CARS distribution deviate significantly from the perfect Gaussian. In particular, we see that the Gaussian approximation is adequate near the peak of the distribution, but becomes completely invalid for improbable events. This deviation may be very significant for applications in which the tails of the distribution are critical, such as data transmission and spectroscopic detection of dilute species. For example, knowledge of the tails may be important for determining the minimum bit error rate (BER) in a CARS wavelength converter or the concentration threshold for detection and identification in CARS spectroscopy. In Fig. 3, we also show the probability distribution for the Stokes output in the case of no input signal (spontaneous emission). In all the plots, the reservoir is taken to be in the ground state.

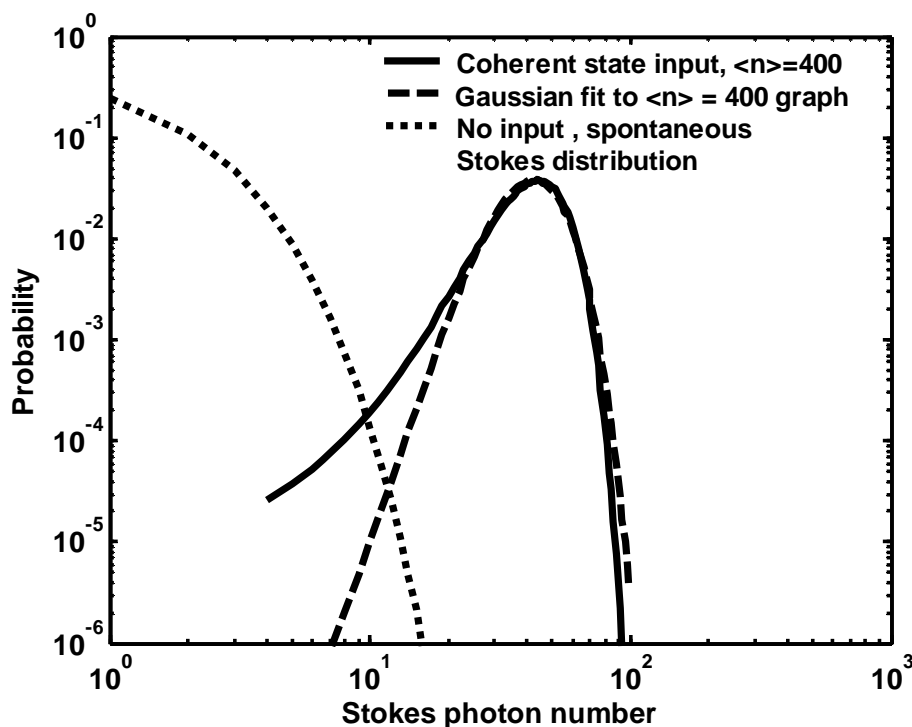


Fig. 3. Photon number probability distribution for the Stokes output with an anti-Stokes input of 400 photons (mean number) and a gain parameter $g_s \times L = 0.33$, assuming perfect phase-matching. The mean photon number at the Stokes output is 45; the best fit Gaussian for this mean value is plotted for comparison. The Stokes at the output with no anti-Stokes input is also shown (only spontaneous emission present). The noise reservoir is taken to be in the ground state.

5. Conclusions

We have determined the noise in the CARS process by employing Langevin sources to keep the commutators of the field operators of the Stokes and anti-Stokes waves constant. We have calculated the noise figure and photon statistics for the wavelength conversion processes of Stokes to anti-Stokes and vice versa. The noise in the output Stokes and anti-Stokes fields has two contributions. One part is due to the input zero-point fluctuations coupling to the output and the other part is due to the coupling of the optical fields to the damped material vibrations. The best noise figure achievable is close to the 3 dB noise figure of the optical amplifier with a correction that depends on the ratio of Stokes to anti-Stokes frequencies, the ratio of the indices of refraction at the two frequencies, as well as the ratio of their nonlinear susceptibilities. The photon probability distribution has non-Gaussian tails, which may be significant for applications in data transmission and spectroscopic detection of highly rarified species.

Acknowledgements

The authors would like to thank Dr. J.D. Shah of DARPA/MTO for his support.

Appendix A

We start with the classical propagation equations for the Stokes and anti-Stokes fields, which can be found in standard textbooks of nonlinear optics (see for example [17]):

$$\frac{dA_S}{dx} = g'_S (\omega_S / n_S) |A_P|^2 A_S + \kappa' (\omega_S / n_S) A_P^2 e^{i\Delta\beta x} A_{AS}^* \quad (A1)$$

$$\frac{dA_{AS}^*}{dx} = -\alpha'_{AS} (\omega_{AS} / n_{AS}) |A_P|^2 A_{AS}^* - \kappa' (\omega_{AS} / n_{AS}) (A_P^*)^2 e^{-j\Delta\beta x} A_S, \quad (A2)$$

where A_P , A_S and A_{AS} are the classical amplitudes for the pump, Stokes and anti-Stokes waves respectively; $\Delta\beta = 2\beta_P - \beta_S - \beta_{AS}$ is the wavevector mismatch between the waves (β_j is the propagation constant of the j -th wave, $j = P, S$ or AS); the wave frequencies are denoted by ω_j ; and n_j are the refractive indices. The coefficients in Eqs. (A1) and (A2)

are related to the nonlinear susceptibilities by $g'_S = i \frac{12\pi}{c} \chi_S$, $\alpha'_{AS} = i \frac{12\pi}{c} \chi_{AS}^*$ and $\kappa' = i \frac{12\pi}{c} (\chi_S \chi_{AS}^*)^{1/2}$, where for example $\chi_S \sim \frac{1}{\omega_P - \omega_S - \omega_{VIB} + i\gamma}$. In this context, γ

is the phonon damping coefficient, ω_{VIB} the material vibrational frequency and the Stokes and anti-Stokes frequencies are related by $2\omega_P = \omega_S + \omega_{AS}$. We make the reasonable approximation of small detuning from Raman resonance $\omega_P - \omega_S - \omega_{VIB} \ll \gamma$ so that the susceptibility can be taken to be imaginary for the sake of simplicity.

To obtain the corresponding quantum-field equations, we replace the classical amplitudes with quantum mechanical operators by the substitution $A_j \rightarrow (\omega_j / n_j)^{1/2} \hat{a}_j$. This replacement is similar in purpose to substitutions found in standard textbooks (see for example [18]), but in this case the modes are enumerated in frequency rather than wavevector. This substitution yields the following differential equations for the field operators:

$$\frac{d\hat{a}_S}{dx} = g_S \hat{a}_S + \kappa e^{2j\varphi_P} e^{j\Delta\beta x} \hat{a}_{AS}^+ \quad (A3)$$

$$\frac{d\hat{a}_{AS}^+}{dx} = -\alpha_{AS} \hat{a}_{AS}^+ - \kappa e^{-2j\varphi_P} e^{-j\Delta\beta x} \hat{a}_S, \quad (A4)$$

where φ_P is the phase of the pump wave, $g_S = g'_S \frac{\omega_S}{n_S} |A_P|^2$, $\kappa = \kappa' \left(\frac{\omega_{AS} \omega_S}{n_{AS} n_S} \right)^{1/2} |A_P|^2$

and $\alpha_{AS} = \alpha'_{AS} \frac{\omega_{AS}}{n_{AS}} |A_P|^2$. These operators must obey the usual commutation relationships

$$[\hat{a}_S, \hat{a}_S^+] = 1, [\hat{a}_{AS}, \hat{a}_{AS}^+] = 1 \text{ and } [\hat{a}_S, \hat{a}_{AS}^+] = 0.$$

It is not difficult to see however, that the propagation equations are not consistent with the uncertainty principle. For example, in the absence of coupling between the Stokes and anti-Stokes waves, it is well known that these modes experience only gain and loss, respectively. In this situation, however, the propagation equations displayed above predict that the commutators of the field operators are not conserved: $d[\hat{a}_j, \hat{a}_j^+] / dx \neq 0$. But this is inconsistent with basic quantum theory. The commutator of the field operators determines the noise limit imposed by the uncertainty principle. More specifically, $\langle \Delta \hat{a}_{j,I}^2 \rangle \langle \Delta \hat{a}_{j,Q}^2 \rangle \geq (1/4) \langle [\hat{a}_{j,I}, \hat{a}_{j,Q}] \rangle^2$, where $\hat{a}_{j,I} = (1/2)(\hat{a}_j + \hat{a}_j^+)$ and

$\hat{a}_{j,Q} = (1/2i)(\hat{a}_j - \hat{a}_j^+)$ represent the in-phase and quadrature components of the electromagnetic field. We must modify the propagation equations to include a so-called Langevin noise source operator, which restores the commutator to a constant value, i.e., $d[\hat{a}_{j,I}, \hat{a}_{j,Q}]/dx = 0$. The analysis presented here is inspired by the analysis of an optical amplifier in [19]. Since all the terms in the propagation equations are due to coupling of the optical fields with the damped vibrational modes in the material, we need to introduce only one ‘noise reservoir’ into the propagation equations. As we will show we can obtain consistent results with this approach.

Consider first the equation describing the evolution of the Stokes mode (decoupled from the anti-Stokes) and add a noise source operator \hat{F}_G :

$$d\hat{a}_S/dx = g_S \hat{a}_S + \hat{F}_G. \quad (A5)$$

The commutator conservation equation gives the condition: $[\hat{F}_G, \hat{a}_S^+] + [\hat{a}_S, \hat{F}_G^+] = -2g_S$. The noise operator and the field operator do not commute. The inhomogeneous solution of the propagation equation gives:

$$\hat{a}_S^{INH} = \int_{-\infty}^x dx' \exp(g_S(x-x')) \hat{F}_G(x'). \quad (A6)$$

Since the noise is uncorrelated along the propagation, the commutator of the noise source with its conjugate should be proportional to a delta function; thus,

$$[\hat{a}_S^{INH}(x), \hat{F}_G^+(x)] = (1/2)C, \quad (A7)$$

where C is a proportionality constant. In order to satisfy Eq. (A5), we must have $C = -2g_S$ and the noise sources must obey the following commutation relation:

$$[\hat{F}_G(x), \hat{F}_G^+(x')] = -2g_S \delta(x-x'). \quad (A8)$$

Notice that the commutator has a negative value, implying that $\hat{F}_G(x)$ acts as a creation operator and $\hat{F}_G^+(x)$ as an annihilation operator for ‘noise reservoir’ excitations. To make the correspondence more explicit we rename the noise source operator: $\hat{F}_G(x) = \exp(j\theta_S) \sqrt{2g_S} \hat{N}^+(x)$, where $\hat{N}(x)$ and $\hat{N}^+(x)$ are now standard annihilation and creation operators with $[\hat{N}(x), \hat{N}^+(x')] = \delta(x-x')$ and $\exp(j\theta_S)$ is an undetermined phase factor whose purpose will become clear below. In a similar manner, we can also show that for the decoupled anti-Stokes mode, the noise source $\hat{F}_L(x) = \exp(-j\theta_{AS}) \sqrt{2\alpha_{AS}} \hat{N}(x)$ is required.

If the Stokes and anti-Stokes modes are coupled, we must also require that $d[\hat{a}_S, \hat{a}_{AS}^+]/dx = 0$ and $d[\hat{a}_S, \hat{a}_{AS}]/dx = 0$. It is not difficult to see that the first condition is satisfied using the previous expressions. The purpose of the explicit phase factors included above becomes clear when we examine the second condition. Although the values of these phase factors have no impact on the previous condition (as long as θ_S and θ_{AS} are real), they must be constrained to satisfy the second condition. Inserting the renamed noise operators into the equations of propagation and requiring $d[\hat{a}_S, \hat{a}_{AS}]/dx = 0$, we obtain the condition:

$$\begin{aligned} & \kappa e^{j(\Delta\beta x + 2\phi_p)} [\hat{a}_{AS}^+, \hat{a}_{AS}] - \kappa e^{j(\Delta\beta x + 2\phi_p)} [\hat{a}_S, \hat{a}_S^+] \\ & + \exp(j\theta_S) \sqrt{2g_S} [\hat{N}^+, \hat{a}_{AS}] + \exp(-j\theta_{AS}) \sqrt{2\alpha_{AS}} [\hat{a}_S, \hat{N}] = 0. \end{aligned} \quad (A9)$$

We can evaluate the last two commutators in this expression using the inhomogeneous solution of the propagation equations:

$$\hat{a}_S(x) = \exp(j\theta_S) \sqrt{2g_S} \int_0^x dx' P_S(x-x') \hat{N}^+(x') \quad (\text{A10})$$

$$\hat{a}_{AS}^+(x) = \exp(j\theta_{AS}) \sqrt{2\alpha_{AS}} \int_0^x dx' P_{AS}(x-x') \hat{N}^+(x'), \quad (\text{A11})$$

where in the above expressions $P_S(0) = P_{AS}(0) = 1$. The functions $P_S(x)$ and $P_{AS}(x)$ are calculated explicitly in Appendix B (see equations (B9) and (B10)). Inserting (A10) and (A11) in (A9) we obtain:

$$\theta_S - \theta_{AS} = \Delta\beta x + 2\varphi_P + \pi, \quad (\text{A12})$$

where we have incorporated the relations, $\alpha_{AS} = r^2 g_S$ and $\kappa = r g_S$ in the last step, with

$$r = \frac{\omega_{AS} n_S (\chi_{AS}^* / \chi_S)^{1/2}}{\omega_S n_{AS}}. \quad \text{In what follows, we choose } \theta_S = -\pi/2 \quad \text{and}$$

$\theta_{AS} = -\Delta\beta \cdot x - 2\varphi_P - (3\pi/2)$ without loss of generality. Our final equations are:

$$\frac{d\hat{a}_S}{dx} = g_S \hat{a}_S + r g_S \exp(j(\Delta\beta x + 2\varphi_P)) \hat{a}_{AS}^+ - j\sqrt{2g_S} \hat{N}^+ \quad (\text{A13})$$

$$\begin{aligned} \frac{d\hat{a}_{AS}^+}{dx} &= -r^2 g_S \hat{a}_{AS}^+ - r g_S \exp(-j(\Delta\beta \cdot x + 2\varphi_P)) \hat{a}_S \\ &+ j \exp(-j(\Delta\beta \cdot x + 2\varphi_P)) \sqrt{2r^2 g_S} \hat{N}^+. \end{aligned} \quad (\text{A14})$$

Appendix B

Here we derive the solution to the coupled differential equations (1a) and (1b) for the Stokes and anti-Stokes field operators. In Eqs. (1a) and (1b) we make the substitutions:

$$\hat{a}_S = \hat{b}_S \exp(j\Delta\beta x / 2), \quad \hat{a}_{AS}^+ = \hat{b}_{AS}^+ \exp(-j\Delta\beta x / 2). \quad (\text{B1})$$

This yields:

$$\frac{d}{dx} \hat{b}_S = (g_S - j(\Delta\beta/2)) \hat{b}_S + r g_S \theta \hat{b}_{AS}^+ - j\sqrt{2g_S} e^{-j\Delta\beta x/2} \hat{N}^+(x) \quad (\text{B2})$$

$$\begin{aligned} \frac{d}{dx} \hat{b}_{AS}^+ &= (j(\Delta\beta/2) - r^2 g_S) \hat{b}_{AS}^+ - r g_S \theta^* \hat{b}_S \\ &+ j \theta^* e^{-j\Delta\beta \cdot x/2} \sqrt{2r^2 g_S} \hat{N}^+(x), \end{aligned} \quad (\text{B3})$$

where $\theta = \exp(j2\varphi_P)$.

It is easy to see that the linear combinations:

$$\hat{U}_{(+)} = \hat{b}_S + C_{(+)} \hat{b}_{AS}^+, \quad \hat{U}_{(-)} = \hat{b}_S + C_{(-)} \hat{b}_{AS}^+, \quad (\text{B4})$$

with

$$C_{(\pm)} = \frac{((r^2 + 1)g_S - i\Delta\beta) \pm \sqrt{((r^2 + 1)g_S - i\Delta\beta)^2 - 4r^2 g_S^2}}{2r g_S} \theta, \quad (\text{B5})$$

obey the following equations:

$$\frac{d}{dx} \hat{U}_{(\pm)} = \Lambda_{(\pm)} \hat{U}_{(\pm)} + j\sqrt{2g_S} (r\theta^* C_{(\pm)} - 1) e^{-j\Delta\beta \cdot x/2} \hat{N}^+(x), \quad (\text{B6})$$

where $C_{(\pm)} = (g_S - i(\Delta\beta/2) - \Lambda_{(\pm)})\theta / (r g_S)$ or

$$\Lambda_{(\pm)} = \frac{g_s(1-r^2) \mp \sqrt{(g_s(1+r^2) - i\Delta\beta)^2 - 4r^2 g_s^2}}{2}. \quad (\text{B7})$$

The solution of Eq. (B6) is:

$$\hat{U}_{(\pm)}(x) = \exp(\Lambda_{(\pm)}x) \hat{U}_{(\pm)}(0) + j\sqrt{2g_s}(r\theta * C_{(\pm)} - 1) \int_0^x dx' \exp(\Lambda_{(\pm)}(x-x')) e^{-j\Delta\beta \cdot x'/2} \hat{N}^+(x'). \quad (\text{B8})$$

Using Eq. (B4) we find the final expressions for the Stokes and anti-Stokes operators:

$$\begin{aligned} \hat{b}_s(x) &= \frac{C_{(-)} \exp(\Lambda_{(+)}x) - C_{(+)} \exp(\Lambda_{(-)}x)}{C_{(-)} - C_{(+)}} \hat{b}_s(0) \\ &+ C_{(-)} C_{(+)} \frac{\exp(\Lambda_{(+)}x) - \exp(\Lambda_{(-)}x)}{C_{(-)} - C_{(+)}} \hat{b}_{AS}^+(0) \\ &+ j\sqrt{2g_s} \int_0^x dx' \left[\frac{(r\theta * C_{(+)} - 1) C_{(-)} \exp(\Lambda_{(+)}(x-x'))}{C_{(-)} - C_{(+)}} \right. \\ &\quad \left. - \frac{(r\theta * C_{(-)} - 1) C_{(+)} \exp(\Lambda_{(-)}(x-x'))}{C_{(-)} - C_{(+)}} \right] e^{-j\Delta\beta \cdot x'/2} \hat{N}^+(x'), \end{aligned} \quad (\text{B9})$$

$$\begin{aligned} \hat{b}_{AS}^+(x) &= \frac{\exp(\Lambda_{(+)}x) - \exp(\Lambda_{(-)}x)}{C_{(+)} - C_{(-)}} \hat{b}_s(0) \\ &+ \frac{C_{(+)} \exp(\Lambda_{(+)}x) - C_{(-)} \exp(\Lambda_{(-)}x)}{C_{(+)} - C_{(-)}} \hat{b}_{AS}^+(0) \\ &+ j\sqrt{2g_s} \int_0^x dx' \left[\frac{(r\theta * C_{(+)} - 1) \exp(\Lambda_{(+)}(x-x'))}{C_{(+)} - C_{(-)}} \right. \\ &\quad \left. - \frac{(r\theta * C_{(-)} - 1) \exp(\Lambda_{(-)}(x-x'))}{C_{(+)} - C_{(-)}} \right] e^{-j\Delta\beta \cdot x'/2} \hat{N}^+(x'). \end{aligned} \quad (\text{B10})$$

Substituting Eqs. (B9) and (B10) into Eqs. (B1) we find the solution for the field operators \hat{a}_s and \hat{a}_{AS}^+ . The parameters A , B , C and D that appear throughout the main text are then given by the respective coefficients of the equations.

Appendix C

Here we derive the expression given above for the photon number probability distribution in CARS wavelength conversion. To calculate the probability distribution, we must determine its characteristic function defined as the Fourier series of the probability distribution:

$$\tilde{P}(k) = \sum_{n=0}^{\infty} p(n) e^{-jkn} = \langle e^{-jkn} \rangle, \quad (\text{C1})$$

which is also the expectation value of e^{-jkn} where n is the photon number. The probability distribution is expressed in terms of the characteristic function as:

$$p(n_o) = \frac{1}{2\pi} \int_0^{2\pi} dk e^{jkn_o} \langle e^{-jkn} \rangle. \quad (\text{C2})$$

We present the calculation of the characteristic function for anti-Stokes to Stokes conversion; the derivation for Stokes to anti-Stokes conversion proceeds in a similar fashion. Also we take the reservoir to be in the ground state. The case where the reservoir is in a thermal state is slightly more complicated to compute but similar to the calculation below.

The characteristic function to be evaluated is:

$$\langle \exp(-jk\hat{a}_s^+(x)\hat{a}_s(x)) \rangle = {}_R \langle 0|_{AS} \langle a|_S \langle 0| \exp(-jk\hat{a}_s^+(x)\hat{a}_s(x)) |0\rangle_S |a\rangle_{AS} |0\rangle_R. \quad (C3)$$

We will need the expansion of the exponential with the operators put in normal and in anti-normal order:

$$\exp(-\xi\hat{a}^+\hat{a}) = \sum_{n=0}^{\infty} \frac{(e^{-\xi} - 1)^n}{n!} (\hat{a}^+)^n \hat{a}^n, \quad (C4)$$

$$\exp(-\xi\hat{a}\hat{a}^+) = e^{\xi} \sum_{n=0}^{\infty} \frac{(1 - e^{\xi})^n}{n!} \hat{a}^n (\hat{a}^+)^n. \quad (C5)$$

These results can be found for example in [20]. Next, we compute $\langle (\hat{a}_s(x))^n (\hat{a}_s^+(x))^n \rangle$. The expectation value is given by:

$${}_R \langle 0|_{AS} \langle a|_S \langle 0| (\hat{a}_s(x))^n (\hat{a}_s^+(x))^n |0\rangle_S |a\rangle_{AS} |0\rangle_R = \sum_{l=0}^n \binom{n}{l} \frac{n!}{l!} |Ba|^l |A|^{2(n-l)},$$

where we have used the binomial expansion and kept only surviving terms. If we substitute the relations $\eta = |A|^2$ and $\xi' = |Ba|^2 / \eta$ into the previous expression, we can rewrite it as:

$$\sum_{l=0}^n \binom{n}{l} n(n-1)\dots(l+1) (\xi')^l \eta^n = \eta^n \sum_{l=0}^n \binom{n}{l} \frac{\partial^{n-l}}{\partial \xi'^{n-l}} (\xi')^n = \eta^n \left(1 + \frac{\partial}{\partial \xi'}\right)^n (\xi')^n.$$

The characteristic function can now be expressed as:

$$\begin{aligned} \langle \exp(-\xi\hat{a}_s^+(x)\hat{a}_s(x)) \rangle &= e^{\xi} \sum_{n=0}^{\infty} \frac{(1 - e^{\xi})^n}{n!} \langle \hat{a}_s(x)^n (\hat{a}_s^+(x))^n \rangle \\ &= e^{\xi} \sum_{n=0}^{\infty} \frac{(1 - e^{\xi})^n}{n!} \eta^n \left(1 + \frac{\partial}{\partial \xi'}\right)^n (\xi')^n. \end{aligned}$$

Next, considering $1 + \partial / \partial \xi'$ and ξ' as operators we note that $[1 + \partial / \partial \xi', \xi'] = 1$ so that they have the same commutation relationship as \hat{a} and \hat{a}^+ . We define a new variable ξ'' as $\eta - \eta e^{\xi} = 1 - e^{\xi''}$, which we use to rewrite the characteristic function:

$$\begin{aligned} \langle \exp(-\xi\hat{a}_s^+(x)\hat{a}_s(x)) \rangle &= \frac{e^{\xi''} + \eta - 1}{\eta} \sum_{n=0}^{\infty} \frac{(1 - e^{\xi''})^n}{n!} \left(1 + \frac{\partial}{\partial \xi'}\right)^n (\xi')^n \\ &= \frac{1 + (\eta - 1)e^{-\xi''}}{\eta} \exp(-\xi'' \xi' (1 + \partial / \partial \xi')). \end{aligned}$$

Next we utilize the normal form of the exponential of $\xi'(1 + \partial / \partial \xi')$, which gives:

$$\begin{aligned} \langle \exp(-\xi\hat{a}_s^+(x)\hat{a}_s(x)) \rangle &= \frac{1 + (\eta - 1)e^{-\xi''}}{\eta} \sum_{n=0}^{\infty} \frac{(e^{-\xi''} - 1)^n}{n!} (\xi')^n (1 + \partial / \partial \xi')^n \\ &= \frac{1 + (\eta - 1)e^{-\xi''}}{\eta} \sum_{n=0}^{\infty} \frac{(e^{-\xi''} - 1)^n}{n!} (\xi')^n \\ &= \frac{1 + (\eta - 1)e^{-\xi''}}{\eta} \exp(-\xi' (1 - e^{-\xi''})). \end{aligned}$$

Finally, substituting ξ'' and setting $\xi = jk$ we obtain the characteristic function in closed form:

$$\langle \exp(-jk\hat{a}_S^+(x)\hat{a}_S(x)) \rangle = e^{-\xi'} \frac{e^{jk}}{1+\eta(e^{jk}-1)} \exp\left(\frac{\xi'}{1+\eta(e^{jk}-1)}\right). \quad (\text{C6})$$

As previously stated, the probability that the photon number $\hat{a}_S^+(x)\hat{a}_S(x)$ has a value n_o given a coherent state with amplitude a as the input is given by the Fourier transform of the characteristic function. To compute the transform, we rewrite the integral obtained from Eqs. (C2) and (C6) by changing to the variable $z = e^{jk}$:

$$p(n_o | a) = e^{-\xi'} \int \frac{dz}{2\pi i} \frac{z^{n_o}}{(z - z_o)} \exp\left(\frac{\xi'/\eta}{z - z_o}\right), \quad (\text{C7})$$

where $z_o = (\eta - 1)/\eta$ and the integrand has a pole at $z = z_o$. To evaluate this integral, we expand the exponential and carry out the integration in the complex plane of every term in the expansion. The result is:

$$p(n_o | a) = e^{-\xi'} \sum_{n=0}^{\infty} \frac{(\xi'/\eta)^n}{\eta n!} \int \frac{z^{n_o} dz}{2\pi i (z - z_o)^{n+1}} = e^{-\xi'} \sum_{n=0}^{n_o} \binom{n_o}{n} \frac{(\xi'/\eta)^n}{\eta n!} z_o^{n_o-n}. \quad (\text{C8})$$

This is the distribution we are seeking.